Once you have Acrobat Reader open on your computer, click on the Comment tab at the right of the toolbar:

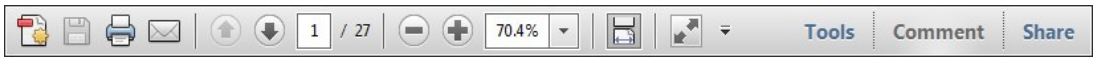

This will open up a panel down the right side of the document. The majority of tools you will use for annotating your proof will be in the Annotations section, pictured opposite. We've picked out some of these tools below:

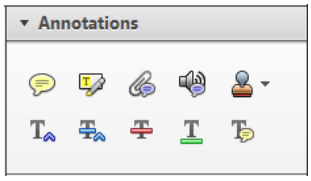

1. Replace (Ins) Tool – for replacing text.

Strikes a line through text and opens up a text box where replacement text can be entered.

How to use it

- Highlight a word or sentence.
- Click on the Replace (Ins) icon in the Annotations section.
- Type the replacement text into the blue box that appears.

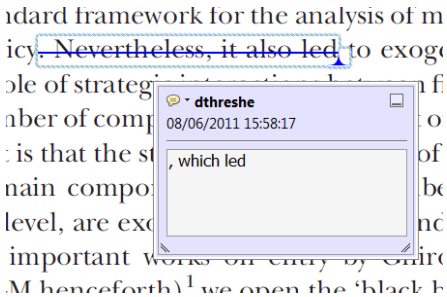

2. Strikethrough (Del) Tool – for deleting text.

Strikes a red line through text that is to be deleted.

How to use it

- Highlight a word or sentence.
- Click on the Strikethrough (Del) icon in the Annotations section.

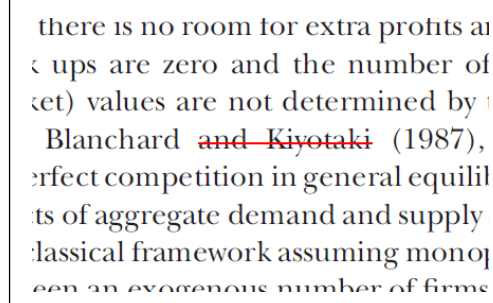

3. Add note to text Tool – for highlighting a section to be changed to bold or italic.

Highlights text in yellow and opens up a text box where comments can be entered.

How to use it

- Highlight the relevant section of text.
- Click on the Add note to text icon in the Annotations section.
- Type instruction on what should be changed regarding the text into the yellow box that appears.

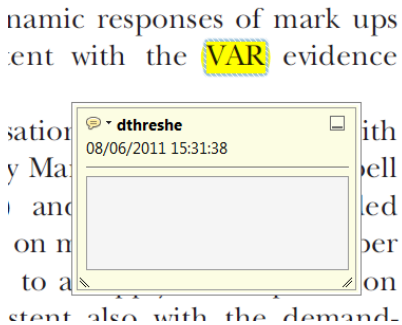

4. Add sticky note Tool – for making notes at specific points in the text.

Marks a point in the proof where a comment needs to be highlighted.

How to use it

- Click on the Add sticky note icon in the Annotations section.
- Click at the point in the proof where the comment should be inserted.
- Type the comment into the yellow box that appears.

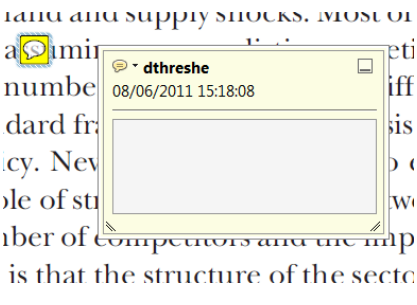

5. Attach File Tool – for inserting large amounts of text or replacement figures.

Inserts an icon linking to the attached file in the appropriate place in the text.

How to use it

- Click on the Attach File icon in the Annotations section.
- Click on the proof to where you'd like the attached file to be linked.
- Select the file to be attached from your computer or network.
- Select the colour and type of icon that will appear in the proof. Click OK.

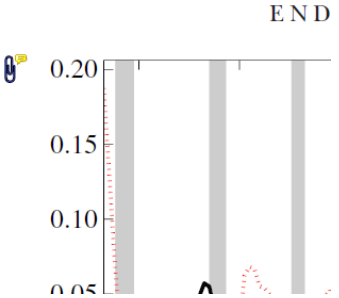

6. Drawing Markups Tools – for drawing shapes, lines and freeform annotations on proofs and commenting on these marks.

Allows shapes, lines and freeform annotations to be drawn on proofs and for comment to be made on these marks.

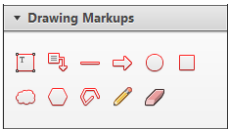

How to use it

- Click on one of the shapes in the Drawing Markups section.
- Click on the proof at the relevant point and draw the selected shape with the cursor.
- To add a comment to the drawn shape, move the cursor over the shape until an arrowhead appears.
- Double click on the shape and type any text in the red box that appears.

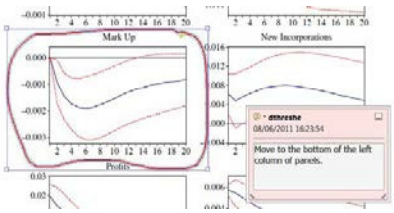

A pathogenic long noncoding RNA redesigns the epigenetic landscape of the infected cells by subverting host Histone Deacetylase 6 activity

Mayte Castellano, Vicente Pallas and Gustavo Gomez

Instituto de Biología Molecular y Celular de Plantas (IBMCP), Consejo Superior de Investigaciones Científicas (CSIC)-Universidad Politecnica de Valencia (UPV), CPI, Edificio 8 E, Av. de los Naranjos s/n, Valencia 46022, Spain

Author for correspondence:
Gustavo Gomez
Tel: +34 963877877
Email: ggomez@ibmcp.upv.es

Received: *4 March 2016*
Accepted: *5 April 2016*

New Phytologist (2016)
doi: 10.1111/nph.14001

Key words: DNA methylation, epigenetic plant response to infections, viroid–host interaction, viroid-induced pathogenesis, viroid–protein interactions.

Summary

- Viroids – ancient plant-pathogenic long noncoding RNAs – have developed a singular evolutionary strategy based on reprogramming specific phases of host-metabolism to ensure that their infection cycle can be completed in infected cells. However, the molecular aspects governing this transregulatory phenomenon remain elusive.
- Here, we use immunoprecipitation assays and bisulfite sequencing of rDNA to shown that, in infected cucumber and *Nicotiana benthamina* plants, *Hop stunt viroid* (HSVd) recruits and functionally subverts Histone Deacetylase 6 (HDA6) to promote host-epigenetic alterations that trigger the transcriptional alterations observed during viroid pathogenesis.
- This notion is supported by the demonstration that, during infection, the HSVd–HDA6 complex occurs *in vivo* and that endogenous HDA6 expression is increased in HSVd-infected cells. Moreover, transient overexpression of recombinant HDA6 reverts the hypomethylation status of rDNA observed in HSVd-infected plants and reduces viroid accumulation. We hypothesize that the host-transcriptional alterations induced as a consequence of viroid-mediated HDA6 recruitment favor spurious recognition of HSVd-RNA as an RNA Pol II template, thereby improving viroid replication.
- Our results constitute the first description of a physical and functional interaction between a pathogenic RNA and a component of the host RNA silencing mechanism, providing novel evidence of the potential of these pathogenic lncRNAs to physically redesign the host-cell environment and reprogram their regulatory mechanisms.

Introduction

Viroids are a class of subviral plant pathogenic long noncoding RNAs (lncRNAs) composed of a circular, single-stranded (240–400 nt in length) molecule (Flores *et al.*, 2014; Palukaitis, 2014; Katsarou *et al.*, 2015). Limited by their nature as obligate intracellular parasites, viroids must optimize their minimum nonprotein-coding genome to ensure autonomous proliferation within infected hosts (Ding, 2010). To overcome this challenge, these lncRNAs have evolved through their adaptive history into versatile molecules that are able to subvert specific plant cell components and/or mechanisms at different functional levels (Navarro *et al.*, 2012a,b; Gago-Zachert, 2016). A representative example of this ability can be observed in the generation of their progeny. Replication of viroids in the nucleus (for members of the family *Pospiviroidae*) or chloroplasts (for members of the family *Avsunviroidae*) is a sequential process that involves transcription, cleavage and circularization of RNA strands. An increasing body of evidence has demonstrated that, besides recruiting cellular mechanisms commonly involved in host RNA metabolism (Navarro *et al.*, 2000; Gas *et al.*, 2007; Nohales *et al.*, 2012a,b), viroids are able to subvert and redirect DNA-dependent factors such as DNA-dependent RNA Polymerase II (RNA Pol II) (Flores & Semancik, 1982; Mühlbach & Sänger, 1997) and/or DNA ligase 1 (Nohales *et al.*, 2012b) during progeny generation to promote their accumulation in infected cells. However, the strategy used by these pathogenic lncRNAs to reprogram the activity of the cellular components involved in host RNA and/or DNA processing is currently unknown.

The functional alterations induced by viroids in infected plants – more commonly recognized as symptoms – represent another aspect of the infection cycle that is intimately associated with the ability of viroids to interfere with host cell homeostasis. Although the basis of viroid pathogenesis remains to be fully deciphered, this process can be envisioned as the product of diverse disruptions in plant gene expression generated by viroid interference in ncRNA-directed regulatory networks (Owens & Hammond, 2009; Navarro *et al.*, 2012a,b; Gomez & Pallas, 2013; Palukaitis, 2014; Gago-Zachert, 2016). In recent years, several studies have provided evidence for the existence of a close interplay between

Journal Code N P H
Manuscript No. 14001 / 2016-21561
WILEY
Dispatch: 29.4.16
No. of pages: 12
CE: Raja
PE: Vigneswari
Color:

viroid-induced pathogenesis and RNA silencing. The idea that viroid-derived sRNAs (vd-sRNAs) can trigger the post-transcriptional cleavage of host mRNAs and induce the expression of plant symptoms (Papaefthimiou *et al.*, 2001; Wang *et al.*, 2004; Gomez *et al.*, 2009) was validated experimentally for viroids that replicate in the nucleus (Gomez *et al.*, 2008; Eamens *et al.*, 2014; Adkar-Purushothama *et al.*, 2015) and chloroplasts (Navarro *et al.*, 2012b). However, the recent observation that *Hop stunt viroid* (HSVd) infection is associated with decreased levels of methylation for normally silenced host genes (Martinez *et al.*, 2014; Castellano *et al.*, 2015) opened the door to the notion that the viroid interference of plant gene expression is a multilayered process, which may also include epigenetic alterations in host gene expression (Castellano *et al.*, 2015; Dalakouras *et al.*, 2015).

Experiments in two different hosts (cucumber (*Cucumis sativus*) and *Nicotiana benthamiana*) have shown that HSVd-infected plants overaccumulate ribosomal-derived sRNAs (rb-sRNAs) as a consequence of increased transcriptional activity of rRNA precursors. This phenomenon correlated with a significant reduction in the methylation levels of ribosomal DNA (rDNA) promoter regions, providing evidence that specific rRNA genes commonly silenced by cytosine methylation are transcriptionally reactivated during viroid infection (Martinez *et al.*, 2014; Castellano *et al.*, 2015). These results suggest that HSVd infection could be associated with alterations of the epigenetic pathways that regulate the transcription of repetitive rDNA. Intriguingly, the regulatory disorders observed in viroid-infected plants display certain similarities to those described previously in *Arabidopsis* mutants for Histone Deacetylase 6 (HDA6). The *hda6* mutants lose the maintenance of symmetric methylation of 45S rRNA promoter regions, which increases their transcriptional activity in parallel with massive overproduction of rb-sRNAs (Earley *et al.*, 2010), resembling, at least in part, the observations in HSVd-infected plants. In *Arabidopsis,* HDA6, a class I RPD3-like HDAC, is recognized as a component of the plant-specific gene silencing mechanism called RNA-directed DNA methylation (RdDM) (Dalakouras & Wassenegger, 2013). Increasing evidence indicates that HDA6 is an epigenetic regulator involved in the maintenance and *de novo* DNA methylation of Transposable Elements (TEs), rRNA genes and transgenes (Aufsatz *et al.*, 2002; Probst *et al.*, 2004; May *et al.*, 2005; To *et al.*, 2011; Liu *et al.*, 2012a,b; Hristova *et al.*, 2015) via interactions with Methyltransferase 1 (MET1). The similarity between the regulatory disturbances observed in HSVd-infected plants and *hda6* mutants prompted us to speculate that viroid-induced interferences in the regulatory pathways mediated by HDA6 could be linked to the epigenetic alterations observed in HSVd-infected plants.

In order to provide experimental evidence to support this hypothesis, we analyzed the possible interrelation between HSVd infection and HDA6 in both cucumber and *N. benthamiana* plants. Our results reveal that viroid infection is associated with overaccumulation of HDA6 in the natural HSVd–host cucumber. In parallel, we demonstrate that HSVd RNA is able to bind HDA6 *in vitro* and confirmed that this interrelation also occurs *in vivo* during viroid infection. Regarding the functional aspects of the interaction between HSVd and HDA6, the data obtained by bisulfite sequencing demonstrated that transient overexpression of recombinant HDA6 in infected plants reversed the hypomethylation of the ribosomal genes induced by viroid infection, directly linking viroid-mediated recruitment of HDA6 and loss of methylation maintenance. Moreover, we provide evidence of an inverse correlation between transient expression of HDA6 and HSVd accumulation in both cucumber and *N. benthamiana* hosts, suggesting that the recruitment of this protein to the HSVd-HDA6 complex, which we observed *in vivo*, may play a crucial role in viroid accumulation in infected plants.

Materials and Methods

Plant material

Twelve-day-old cucumber (*Cucumis sativus* L cv Suyo*)* and 20-d-old *Nicotiana benthamiana* Domin plants were agro-inoculated with the *Agrobacterium tumefaciens* strain C58C1 transformed with a binary pMOG800 vector carrying a head-to-tail infectious dimeric *Hop stunt viroid* (HSVd) cDNA (Y09352) (Gomez & Pallas, 2006) or an empty vector in both cotyledons and basal leaves. Plants were maintained in growth chambers at 28°C for 16 h with fluorescent light and at 24°C for 8 h in darkness. Plants were analyzed as described in the figure legends. The HSVd/Nb plants (Gomez & Pallas, 2006) used in this study that carry a dimeric sequence of HSVd are able to process, accumulate and systemically transport viroid mature forms. Untransformed and HSVd/Nb plants were maintained in growth chambers (16 h light : 8 h dark, 28°C day : 24°C night) for 6–7 wk.

Expression and purification of recombinant HDA6

The putative cucumber Histone Deacetylase 6 (HDA6) was amplified by RT-PCR using the SuperScript® III One-Step RT-PCR System with Platinum® Taq DNA Polymerase (Invitrogen) according to the manufacturer's instructions. The primers HDA6-DIR: GGATCCATCCGACGACATTCACG and HDA 6-REV: CTCGAGTAAGAAGTATGGCTTGATCCTAG carrying the *Bam*HI and *Xho*I restriction sites, respectively, were used for amplification. The amplified fragments were cloned and sequenced. After establishing the correct cucumber HDA6 sequence, HDA6-ORF was *Bam*HI and *Xho*I digested and cloned into the expression vector pETDue-1 (Novagen) to obtain a recombinant version of HDA6 including amino-terminal Met-Gly-Ser-Ser-His6 extensions. The recombinant protein was purified under denaturing conditions by chromatography using a 1-ml Ni-NTA Agarose column (NI-NTA Purification System; Invitrogen) according to the manufacturer's instructions. The purified recombinant HDA6 protein was used to generate polyclonal antiserum in rabbits as described previously (Gomez & Pallas, 2004) and to perform HSVd-RNA binding assays by Northwestern blot.

Western blot assays

Protein extracts obtained from cucumber and *N. benthamiana* were fractionated by SDS-PAGE 12% and transferred to PVDF membranes. Membranes were treated for 1 h in blocking solution (TBS (500 mM NaCl, 20 mM Tris, pH 7.5), 5% defatted milk, 2% BSA, and 0.1% Triton X-100) and incubated overnight with the antiserum against cucumber HDA6 or Green Fluorescent Protein (GFP) accordingly. Membranes were washed (TBS, 0.5% Tween 20), incubated with anti-rabbit IgG linked to horseradish peroxidase whole antibody. The antibody-protein complex was detected by luminescence (ECL+Plus; Amersham-Pharmacia Biotech, Amersham, UK) according to the manufacturer's instructions. The serological detection of nuclear and cytoplasmic protein controls was performed with antisera against Histone 3 (H3) and UDP-glucose pyrophosphorylase (UDP) (Agrisera AB, Vannas, Sweden – AS10710 and AS05086, respectively) according to the manufacturer's instructions.

Northwestern blot assays

Recombinant HDA6 was denatured by heating for 5 min at 95°C, fractionated by SDS-PAGE 12% and transferred to nitrocellulose membranes (Bio-Rad). Northwestern assays were performed as described previously (Gomez *et al.*, 2005). Briefly, membranes were incubated in RN Buffer (10 mM Tris-HCl pH 7.5, 1 mM EDTA, 100 mM NaCl, 0.05% Triton X-100, and 1× Denhardt's reagent) for 2 h at room temperature followed by a 3-h incubation in RN buffer in the presence of DIG-labeled HSVd-RNAs (25–50 ng ml^{-1}). The detection of hybrid RNA–protein was performed using a colorimetric method.

Nuclei isolation

The enriched fraction of nuclear proteins was obtained starting from nuclei isolated as described previously (Sikorskaite *et al.*, 2013), with minor modifications. Briefly, tissue extracts were clarified and treated with Triton X-100 to lyse membranes (according to the original protocol). Next, nuclei were collected by centrifugation through 2.5 M sucrose cushion solution (Nuclei Pure Prep Nuclei Isolation Kit; Sigma). In immunoprecipitation (IP) assays, before nuclei isolation, the *N. benthamiana* and cucumber leaves were vacuum infiltrated with 1% formaldehyde to reversibly crosslink the RNA–protein complexes (Ricardi *et al.*, 2010).

Immunoprecipitation assays

Two complementary assays were performed to detect the HDA6–HSVd complexes *in vivo* in *N. benthamiana* and cucumber plants.

N. benthamiana Recombinant HDA6 (carrying an amino-terminal His6 tag) was transiently expressed by agro-infiltration in the leaves of transgenic *N. benthamiana* plants constitutively expressing dimeric HSVd transcripts (HSVd/Nb). Three days after infiltration, the leaves overexpressing HDA6 were treated with 1% formaldehyde to reversibly crosslink the RNA–protein complexes and were used to obtain purified nuclei as described above. The HDA6–HSVd complexes were captured by affinity chromatography with a nickel column (NI-NTA Purification System; Invitrogen) according to the manufacturer's instructions. Eluates were analyzed by Western blot and reverse transcription-polymerase chain reaction (RT-PCR) to detect recombinant HDA6 and HSVd RNA, respectively.

Cucumber Nuclear extracts obtained from the leaves of HSVd-infected plants (at 30 d post inoculation (dpi)) as described above were subjected to conventional IP assays with HDA6-As and agarose-conjugated protein A (Roche Diagnostics) according to the manufacturer's instructions as described previously (Gomez & Pallas, 2004). Immunoprecipitated extracts were analyzed by Western blot and RT-PCR to detect recombinant HDA6 and HSVd-RNA, respectively.

RNA extraction and Northern blot analysis

Total RNAs were extracted using TRI reagent (Sigma) according to the manufacturer instructions. Briefly, 500 mg of leaves from HSVd-infected and control plants were ground in 2 ml of TRI reagent. Then, 400 µl of chloroform was added, and the sample was vigorously vortexed and subsequently centrifuged. The supernatant was recovered, and the total RNAs were precipitated with isopropanol and resuspended in sterile water. The total RNA preparations were quantified by spectrometry and their concentrations were equalized. To analyze the circular and linear forms of HSVd-RNA by Northern blot analysis, 1.5 µg of the total RNA preparations were electrophoresed under denaturing conditions in a 5% polyacrylamide mini-gel, with 0.25 × TBE and 8 M urea. After electrophoresis, the RNAs were blotted onto positively charged nylon membranes and hybridized as described previously (Gomez & Pallas, 2006).

Bisulfite conversion and sequencing

Total genomic DNA was extracted from HSVd-infected and mock-inoculated cucumber and *N. benthamiana* leaves using a protocol described previously (Martinez *et al.*, 2014). Total DNA (1 µg) was diluted into 20 µl of water and subjected to bisulfite treatment using the EpiTect Bisulfite kit (Qiagen) according to the manufacturer's instructions. The rRNA region to be analyzed and the corresponding oligos were determined using MethPrimer software http://www.urogene.org/cgi-bin/methprimer (Li & Dahiya, 2002). PCRs were performed using Taq DNA polymerase (Promega) and analyzed in 1.5% agarose gels. PCR products were purified by gel extraction and cloned using the pTz cloning kit (Fermentas). Twenty to 25 clones were sequenced from each analyzed point from mock-treated and HDA6-expressing HSVd-infected samples. Two independent biological replicates were analyzed for HSVd-infected and mock-inoculated plants.

Agro-infiltration

Nicotiana benthamiana and cucumber plants were infiltrated with the HDA6/GFP or unmodified GFP constructs as described previously (Gomez & Pallas, 2007) and maintained at 28°C with 14 h of light. GFP expression in plants was analyzed at 72 h after agro-infiltration using a TCS SL confocal laser scanning microscope (Leica), with excitation at 488 nm and emission at 510–560 nm. The nuclear localization of the HDA6/GFP was established using Red Fluorescent Protein (RFP) fused to a nucleolar-specific peptide as a reference. The GFP- and HDA6/GFP-expressed proteins were also detected by Western blot using GFP-specific antibodies, as described previously (Gomez & Pallas, 2007).

In transient HDA6 silencing assays, 11-d-old cucumber plants were infiltrated with *Agrobacterium* transformed with the vector hp-HDA6 or empty vector (control) in both cotyledons. At 1 d post agro-infiltration (dpa), the distal part of the cotyledons was inoculated with *Agrobacterium* transformed with a vector carrying a dimeric HSVd cDNA. At 3 dpi with HSVd, the HSVd-inoculated area was eliminated and total RNAs were extracted from the remaining parts of the cotyledons. The RNA was used to determine HSVd accumulation and HDA6 mRNA levels by RT-PCR.

Analysis of GFP expression

GFP expression was analyzed using a Leica MZ 16 F fluorescence stereomicroscope equipped with filters DSR, GFP2 and V (Leica). Tissue sections were also observed using a TCS SL confocal laser scanning microscope (Leica), with excitation at 488 nm and emission at 510–560 nm. GFP was also detected by Western blot using GFP-specific antibodies, as described previously.

Plasmid constructs for RNA silencing assays

A fragment of the cucumber HDA6 sequence between positions 369 and 868 (GenBank accession XM_004138046.2) was inserted in sense orientation between the *Xho*I and *Kpn*I sites and in reverse orientation between the *Xba*I and *Hin*dIII sites of pHANNIBAL (GenBank accession no. AJ311872) to produce a hairpin expression cassette, which included a CaMV 35S promoter and an *A. tumefaciens* ocs terminator. This cassette, flanked by two *Not*I restriction sites, was inserted into the unique *Not*I site of the binary plasmid pMOG. The empty pHANNIBAL *Not*I cassette was also inserted into the binary plasmid pMOG to produce the control plasmid. Both plasmids were electroporated into *A. tumefaciens* C58C1.

RT-PCR analysis

Total RNA was extracted from the leaves of the HSVd-infected and mock-inoculated plants using TRI reagent (Sigma) according to the manufacturer's instructions. RT-PCR analysis was performed using the SuperScript® III One-Step RT-PCR System with Platinum® Taq DNA Polymerase (Invitrogen) according to the conditions described below.

HSVd amplification Primers Dir-1 (GGTTCGCTCCAACC TGCTTTTG) and Rev-1 (CCCCGGGGCTCCTTTCTCA GGT) flanking a ~150 bp region of HSVd RNA. Assay conditions: RT (30 min at 50°C and 3 min at 95°C); 25 PCR cycles at (95°C/15 s, 55°C/20 s, and 70°C/15 s).

25S rRNA amplification Primers 25S-Fw (TATATAAGGG GGGTAGAGGTGTTG) and 25S-Rv (ATRCCAAACACAAC TCACAACAACC) flanking a ~500 bp region of rRNA. Assay conditions: RT (30 min at 50°C and 3 min at 95°C); 20 PCR cycles at (95°C/15 s, 55°C/20 s, and 70°C/30 s).

RuBisCO mRNA amplification Primers Rub-Dir (TACTTG AACGCTACTGCAG) and Rub-Rev (CTGCATGCATTGCA CGGTG) flanking a region (~180 nt) of RuBisCO mRNA were used to amplify this mRNA as a loading control. RT-PCR conditions 45°C for 30 min, followed by 30 cycles of 95°C/15 s, 58°C/20 s, and 70°C/15 s.

Primers H6-Dir (ATGTCCGACGACATTCACGGCG) and H6-Rev (TTTCGGGGCTGACGGAGGCGAG) flanking a region (~280 nt) of cucumber HDA6 mRNA were used to amplify this mRNA. RT-PCR conditions were 45°C for 30 min, followed by 30 cycles of 95°C/15 s, 62°C/20 s, and 70°C/24 s.

Primers Act-Dir (GGAGCTGAGAGATTCCGTTG) and Act-Rev (GGTGCAACGACCTTGATTTT) flanking a region (~270 nt) of cucumber Actin-7 mRNA (XM_004147305.2) were used to amplify this mRNA as a loading control. RT-PCR conditions were 45°C for 30 min, followed by 27 cycles of 95°C/15 s, 57°C/20 s, and 72°C/20 s.

Results

Cucumber HDA6 is a nuclear protein that is overexpressed during HSVd infection

In order to characterize the putative HDA6 protein in cucumber, we first retrieved the predicted HDA6 sequence from GenBank (accession no. XM_004168847.1). Next, starting from a total RNA preparation, we used RT-PCR to amplify the full-length cDNA corresponding to the cucumber HDA6 ORF and cloned the sequence into a plasmid to express a recombinant version of the protein with an amino-terminal His6 tag in *Escherichia coli*. Recombinant HDA6 was purified by affinity chromatography using a nickel column (Supporting Information Fig. S1a) and used to generate a polyclonal antiserum (HDA6-As) in rabbit (Fig. S1b). To evaluate whether the cucumber HDA6 exhibits nuclear localization, like *Arabidopsis* HDA6, we generated a vector expressing the complete HDA6 ORF fused to GFP under the control of the 35S promoter. The HDA6-GFP DNA was cloned into a binary vector to be transformed into *Agrobacterium* and was used for the analysis of transient expression by means of agro-infiltration. Observation of the infiltrated leaves using confocal microscopy revealed that, unlike the free GFP used as a control (detected in the cytosol and the nucleus), the HDA6-GFP was localized mainly in the nuclei of the cucumber (Fig. 1a) and

N. benthamiana (Fig. S2) cells. It is important to note that the predicted size of HDA6-GFP (81 kDa) exceeds the size exclusion limit (40–60 kDa) for passive diffusion of proteins through nuclear pores (Raikhel, 1992). Moreover, specific detection of HDA6 in nuclear fractions recovered from untreated cucumber plants by Western blot assays (Fig. 1c) provided additional evidence supporting that endogenous cucumber HDA6 accumulates in the nucleus. Similar results were obtained in immunological assays performed with nuclear extracts of *N. benthamiana* plants transiently expressing recombinant HDA6 (Fig. S3), reinforcing the confocal microscopy observations and demonstrating that recombinant cucumber HDA6 can accumulate in the nuclei

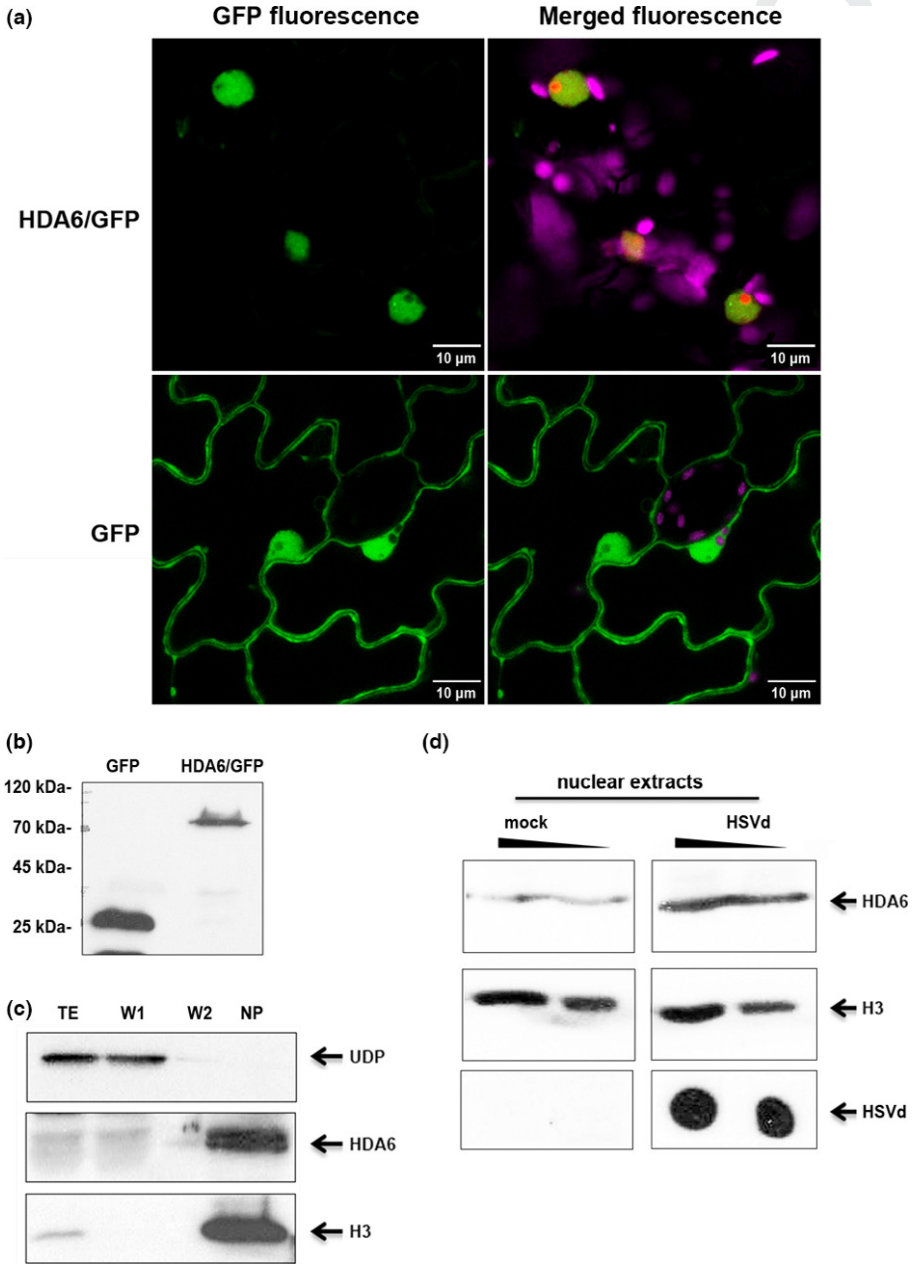

Fig. 1 Cucumber Histone Deacetylase 6 (HDA6) is a nuclear protein that is overexpressed during *Hop stunt viroid* (HSVd) infection. (a) Confocal microscopy imaging of cucumber leaves expressing HDA6/ Green Fluorescent Protein (GFP) (upper panels) and unmodified GFP (lower panels). As can be observed, HDA6/GFP accumulates mainly in the cell nucleus. Fibrillarin fused to Red Fluorescent Protein (RFP) was used as a nucleolar marker. Cell chloroplasts are shown in magenta. (b) The correct expression of the recombinant HDA6/GFP protein in the infiltrated tissues was established by western blotting using anti-GFP. (c) Serological detection (using HDA6-As) of endogenous HDA6 in nuclear extracts of cucumber leaves (middle panel). Histone 3 (H3) (lower panel) and UDP-glucose pyrophosphorylase (UDP) (upper panel) were used as well-established markers of the nuclear and cytoplasmic fractions, respectively. TE, total extract; W1 and W2, Wash 1 and 2, respectively; NP, nuclear pellet. (d) Differential detection of endogenous HDA6 in two dilutions (1 : 1 and 1 : 2) of nuclear extracts from mock-inoculated and HSVd-infected leaves. Accumulation of H3 was assessed as a loading control. The presence of viroid in the infected leaves was confirmed by dot blot hybridization using HSVd-specific probes.

of *N. benthamiana* cells. Next, we reasoned that, as stated in the introduction, a close interaction might occur between HSVd and HDA6 during infection; viroid pathogenesis may be accompanied by alteration in the pattern of HDA6 accumulation in infected cucumber cells. To address this issue, we analyzed the levels of endogenous HDA6 in the nuclear extracts of HSVd-infected and control plants by Western blot. As shown in Figs 1d and S4, viroid infection was associated with increased accumulation of HDA6 in the nuclei of infected cucumber cells, providing evidence of a functional link between HSVd infection and HDA6 metabolism.

HSVd RNA binds to HDA6 *in vitro* and *in vivo*

Keeping in mind that it is generally accepted that viroids use direct interaction as a general mechanism to recruit and subvert host cell factors, we performed *in vitro* assays to determine whether cucumber HDA6 possesses potential HSVd RNA binding activity. Northwestern blot analysis (Gomez *et al.*, 2005) indicated that HDA6 efficiently bound to full-length HSVd transcripts with both plus and minus polarity (Fig. 2a). To complement these data with *in vivo* approaches in a heterologous system, recombinant HDA6 was expressed by agro-infiltration in transgenic *N. benthamiana* plants accumulating HSVd (*HSVd-Nb*) (Gomez & Pallas, 2007). Nuclear extracts were purified from the infiltrated leaves and subjected to capture assays for recombinant HDA6 (carrying an amino-terminal His6 tag) by affinity chromatography using a nickel column. Western blot analysis of the eluates confirmed that recombinant HDA6 could be recovered efficiently from infiltrated leaves (Fig. S5a). The RNAs extracted from the different eluates were subjected to RT-PCR assays to detect viroid RNA and demonstrate that HSVd could be amplified from the eluates containing the HDA6 protein (Fig. S5b). No amplification of HSVd RNA was observed in the eluates recovered from control *HSVd-Nb* leaves infiltrated with *Agrobacterium* carrying the empty vector (Fig. S5b). To provide more robust *in vivo* evidence of the HSVd-HDA6 interaction, we next performed canonical IP assays in infected cucumber plants using the polyclonal antiserum generated against cucumber HDA6 protein (HDA6-As). Immunoprecipitation studies were carried out starting from nuclear extracts (Fig. 2b). When the immunoprecipitates were electrophoresed on SDS-PAGE and analyzed by Western blot assays, we observed that HDA6 was specifically recovered (Fig. 2c). By contrast, no protein bands were detected in the immunoprecipitation control performed with antibody-free protein-A agarose beads (Fig. 2c). The presence of HSVd RNA in the immunoprecipitation extracts was confirmed by RT-PCR. A band of the expected size was only detected in the immunoprecipitation extract containing HDA6 and not in the IP-control lacking HDA6 (Fig. 2c, lower panel).

HDA6 overexpression reverses the hypomethylation induced by HSVd infection

Having confirmed that HSVd interacts directly with HDA6 in infected plants, we next attempted to establish whether this

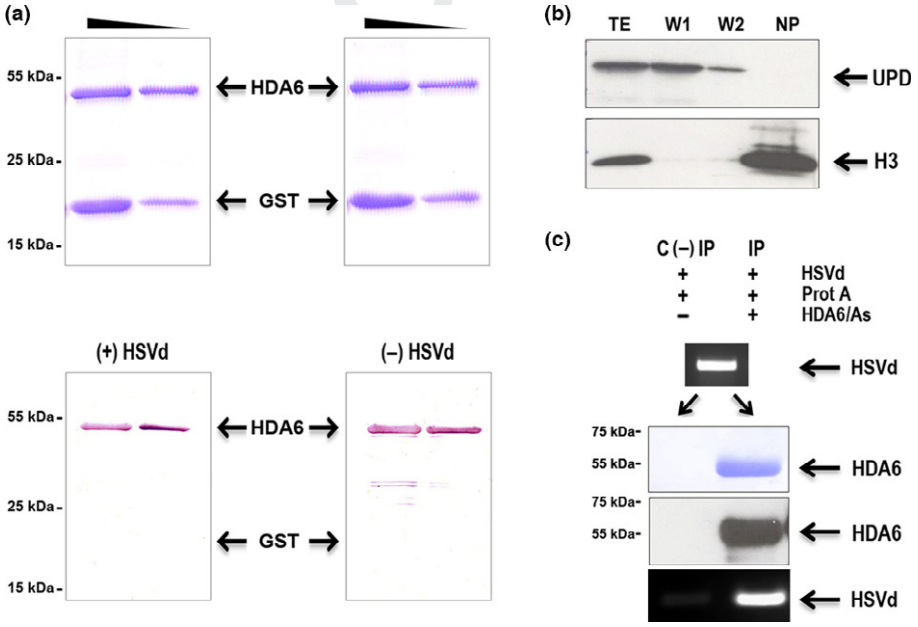

Fig. 2 *Hop stunt viroid*– Histone Deacetylase 6 (HSVd–HDA6) form a stable complex *in vitro* and *in vivo*. (a) Two dilutions (1 and 0.5 μg) of recombinant HDA6 and glutathione S-transferase (GST, used as a control) were subjected to SDS-PAGE (upper panel), transferred to nitrocellulose membranes and analyzed by Northwestern blot with HSVd probes in both (plus and minus) polarities (lower panel left and right, respectively). (b) Purification of nuclear extracts from HSVd-infected cucumber plants. Selective accumulation of Histone 3 (H3) and UDP-glucose pyrophosphorylase (UDP) were used as indicators of enriched cytoplasmic and nuclear fractions (upper and lower panels, respectively). TE, total extract; W1 and W2, Wash 1 and 2, respectively; NP, nuclear pellet. (c) Immunoprecipitation (IP) of HSVd-HDA6 complexes. The nuclear fraction, which was extracted from HSVd-infected plants, was divided into two identical parts. One part was incubated with Protein-A agarose and subjected to IP assays using polyclonal HDA6-As. An equivalent fraction was incubated without HDA6-As as a negative control $C^{(-)}$ IP. The IP of HDA6 was confirmed by SDS-PAGE analysis and serological detection by Western blot (upper panels). Total RNAs extracted from IP fractions were subjected to RT-PCR analysis to confirm the specific recovery of HSVd RNA.

interaction exerts a functional effect on the alteration in the methylation of host DNA observed in HSVd-infected cucumber (Martinez *et al.*, 2014) and *N. benthamiana* (Castellano *et al.*, 2015) plants. First, the time point at which viroid RNA could be detected in systemic leaves of HSVd-inoculated cucumber and *N. benthamiana* plants (Fig. S6a) was determined. Next, we expressed recombinant HDA6 in the apical leaves 3 d before the time point established for HSVd detection. After systemic infection was established, the leaves overexpressing recombinant HDA6 were collected and processed to obtain total RNA and DNA (Fig. S6b,c). The recovered DNA was analyzed by bisulfite sequencing of a region of the cucumber 45S-rDNA promoter (Fig. 3a) containing nine symmetric (five CG, four CHG) and 14 asymmetric (CHH) potential methylation sites (Fig. 3b) that were previously demonstrated to be hypomethylated during HSVd infection (Martinez *et al.*, 2014). Genomic cucumber DNA samples, obtained from HDA6-expressing and control plants, were bisulfite-converted, amplified by PCR and cloned for sequencing. Methylation analysis revealed that, as observed previously (Martinez *et al.*, 2014), HSVd infection decreased the relative number of methylated cytosine residues in cucumber leaves not overexpressing HDA6 compared to noninfected control plants (Fig. 3c). Alterations in methylation were observed in both symmetric and asymmetric sequence contexts (Fig. 3c,d). By contrast, a significant increase in the amounts of total methylated cytosine was observed in HSVd-infected leaves overexpressing recombinant HDA6 in comparison with HSVd-infected leaves without exogenous HDA6 supplementation (Fig. 3c). A detailed analysis showed that this increase in the methylation level was maintained in both symmetric and asymmetric sequence contexts (Fig. 3d). Comparable results regarding cytosine hypomethylation in symmetric sequence contexts were obtained when these assays were performed in conventionally HSVd-infected *N. benthamiana* plants but not in asymmetric sequence contexts (Fig. S7).

HSVd accumulation is affected by HDA6

Our results support the idea that the hypomethylation status associated with HSVd infection could be a consequence of the viroid-mediated recruitment of HDA6 in infected cells, which would explain the disrupted transcriptional scenario observed in

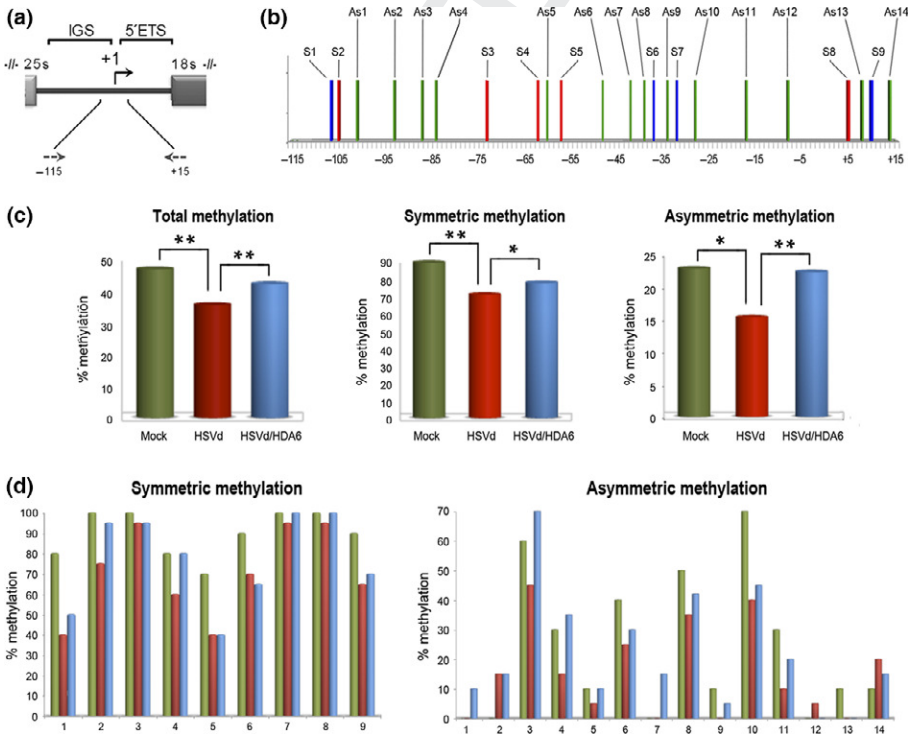

Fig. 3 Histone Deacetylase 6 (HDA6) reverses hypomethylation of the cucumber 45S rRNA gene induced by *Hop stunt viroid* (HSVd) infection. (a) Diagram of the intergenic region of the 45S rRNA highlighting the area of the promoter region analyzed by bisulfite sequencing. The arrows represent the oligos used in the PCR assay and their relative positions in the rRNA. (b) Graphic representation of the potential symmetric (S) and asymmetric (As) methylation positions predicted to exist within the analyzed region. (c) Histogram illustrating the relative DNA methylation levels of the 45S rRNA promoter in cucumber plants: mock-inoculated (green bars), HSVd-infected (red bars) and HSVd-infected plants overexpressing recombinant HDA6 (blue bars). Total methylation (paired *t*-test values) means 0.50 (mock), 0.38 (HSVd) and 0.45 (HSVd/HDA6); **, $P<0.0005$. Symmetric methylation (paired *t*-test values) means 0.88 (mock), 0.70 (HSVd) and 0.77 (HSVd/HDA6); *, $P<0.025$; **, $P<0.0025$. Asymmetric methylation (paired *t*-test values) means 0.24 (mock), 0.16 (HSVd) and 0.23 (HSVd/HDA6); *, $P<0.015$; **, $P<0.0005$. D) Positions of methylcytosines in the analyzed regions displayed in the symmetric (CG and CHG) and asymmetric (CHH) sequence context. The height of the bar represents the frequency at which cytosine was methylated in the three analyzed samples: mock-inoculated (green bars), HSVd-infected (red bars) and HSVd-infected plants overexpressing recombinant HDA6 (blue bars).

the host during HSVd infection (Martinez *et al.*, 2014; Castellano *et al.*, 2015). To clarify whether the HSVd–HDA6 interaction influences viroid accumulation, HSVd presence was analyzed in tissues overexpressing recombinant HDA6 using the RNA extracts obtained from the leaves described above (Fig. S6).

A semi-quantitative RT-PCR assay was used to compare the levels of HSVd in viroid-infected cucumber and *N. benthamiana* plants (Fig. 4a, left and right, respectively). Our data clearly demonstrated that, unlike the endogenous RNAs used as controls, the HSVd accumulation estimated by RT-PCR

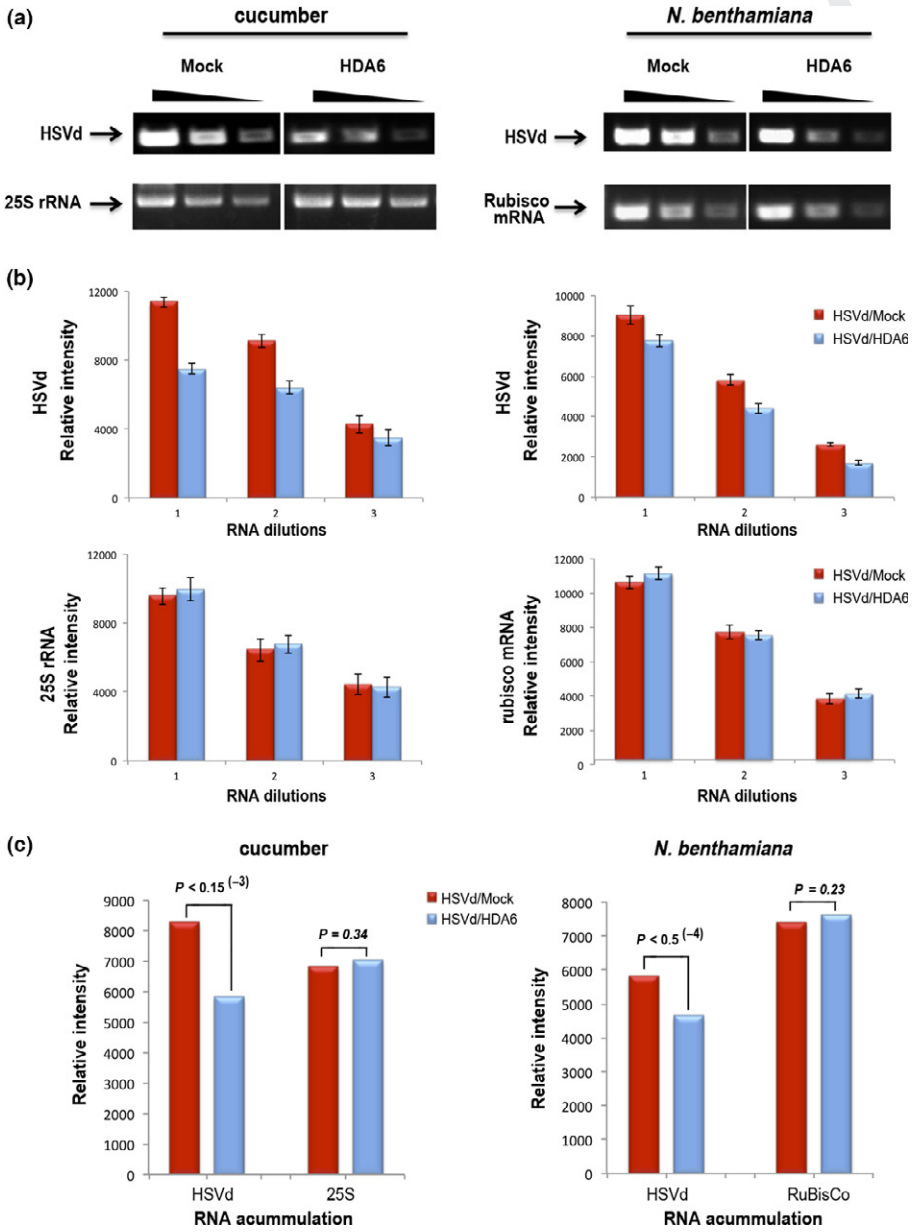

Fig. 4 *Hop stunt viroid* (HSVd) accumulation is negatively affected by Histone Deacetylase 6 (HDA6) overexpression. (a) Representative RT-PCR analyses of the viroid accumulation in serial dilutions of total RNAs extracted from HSVd-infected cucumber (left) and *Nicotiana benthamiana* (right) plants transiently overexpressing recombinant HDA6 or mock infiltrated with empty agrobacterium, as detailed in Supporting Information Fig. S6. RT-PCR amplification of 25S rRNA (cucumber) and RuBisCo mRNA (*N. benthamiana*) served as RNA loading controls. (b) Histogram showing the comparison between the relative intensity of the bands amplified by RT-PCR from the serial dilutions of the RNAs extracted from HSVd/Mock and HSVd/HDA6 plants. The lower panels show the values obtained when the RT-PCR products obtained for 25S and RuBisCo RNAs used as loading controls were analyzed. The bars (red for HSVd/Mock and blue for HSVd/HDA6) represent the means of three biological and three technical replicates for each event, ± SE of the means. (c) Graphical comparison of relative HSVd accumulation levels (estimated from the intensity of the RT-PCR products) in mock-infiltrated and HDA6-overexpressing infected samples. Bars (red for HSVd/Mock and blue for HSVd/HDA6) represent the mean values obtained for HSVd RNA amplification expressed relative to the controls (25S rRNA for cucumber and RuBisCo mRNA for *N. benthamiana* plants). Paired *t*-test values cucumber: HSVd mean values 8258 (mock) and 5801 (HSVd/HDA6); 25 sRNA mean values 6812 (mock) and 7006 (HSVd/HDA6). Paired *t*-test values *N. benthamiana*: HSVd mean values 5822 (mock) and 4602 (HSVd/HDA6); RuBisCo mean values 7412 (mock) and 7615 (HSVd/HDA6). The *P*-values are shown in the figure.

amplification was significantly lower in viroid-infected cucumber (Fig. 4b, left, blue bars) and *N. benthamiana* (Fig. 4b, right, blue bars) leaves overexpressing exogenous HDA6 in comparison with mock-infiltrated HSVd-infected controls (red bars). The observation that viroid accumulation was significantly impaired in both hosts (Fig. 4c), by an excess of HDA6 in the nuclei of the infected cells suggests that recruitment of this host factor during the viroid infective cycle (demonstrated by IP assays) has an influence on the biological efficiency of HSVd.

In order to provide additional evidence for the physiological relevance of the HSVd–HDA6 interaction, we infected cucumber cotyledons overexpressing (by *A. tumefaciens*-mediated transient transformation) a hairpin construct designed to silence the gene encoding cucumber HDA6 (Fig. S8). Total RNA was purified from the infiltrated areas at 3 dpi and analyzed by semi-quantitative RT-PCR assay. The relative accumulation of HSVd was significantly higher in infected cotyledons expressing the HDA6 hairpin construct in comparison with the relative accumulation of HSVd observed in control plants infiltrated with the empty vector (Fig. 5a, b and c). RT-PCR analysis of cucumber HDA6 mRNA indicated a significant reduction at 4 dpi in tissues infiltrated with the hairpin construct relative to those infiltrated with the empty vector (Fig. 5d and e), correlating HDA6-silencing and increasing in HSVd accumulation.

Discussion

Conditioned by their incapacity to encode proteins, it is well established that viroids are strictly dependent on close interactions with host cellular components and functional mechanisms to complete their infection cycle. Considered to be a standardized and unique RNA, viroids have at least two (sequence- and structure-dependent) concomitant flexible ways to interact with plant regulatory machinery. This dual nature provides these long non-coding RNAs (lncRNAs) with the extraordinary potential to subvert plant cell developmental networks at multiple functional levels to increase their biological efficiency (Gomez & Pallas, 2013). Previous observations revealed that *Hop stunt viroid* (HSVd)-infected cucumber and *N. benthamiana* plants exhibited an unexpected decrease in the cytosine methylation levels of the ribosomal gene promoters, demonstrating that HSVd can interfere with specific host methylation pathways during infection in a similar manner as that observed for other plant pathogens (Raja *et al.*, 2008; Dowen *et al.*, 2012; Rodriguez Negrete *et al.*, 2013; Yang *et al.*, 2013; Yu *et al.*, 2013). The similarities between the observations in HSVd-infected plants (hyper-accumulation of 21-nt rb-sRNAs, loss of symmetric methylation and increased ribosomal gene transcription) (Martinez *et al.*, 2014; Castellano *et al.*, 2015) and in mutant *Arabidopsis* plants that fail to express Histone Deacetylase 6 (HDA6) (Earley *et al.*, 2010) provide experimental evidence supporting the possibility that a close interrelationship between HSVd and HDA6 could occur during the pathogenesis process. Our first evidence supporting this idea was the observation that HDA6 accumulation increases in the nuclei of HSVd-infected cucumber cells, thus establishing a functional connection between viroid pathogenesis and HDA6 metabolism in infected plants. Next, *in vitro* assays demonstrated that HSVd RNA could bind recombinant cucumber HDA6, fulfilling the first characteristics essential for the existence of a direct interaction. In this regard, it is important to emphasize that co-compartmentalization of both HSVd–RNA and HDA6 in the nucleus provides a spatial scenario to permit this interaction *in vivo*. Furthermore, the observation that the HDA6–HSVd complex occurred *in vivo* in the heterologous *HSVd-Nb* system provided additional evidence for this interaction. Finally, recovery of the HSVd–HDA6 complex in immunoprecipitation assays of viroid-infected leaves confirmed that HSVd recognizes and recruits endogenous cucumber HDA6 during the pathogenesis process.

Having established the existence of the HSVd–HDA6 complex *in vivo*, we attempted to determine whether this complex possesses a functional relationship with the hypomethylation of rDNA observed during viroid infection (Martinez *et al.*, 2014; Castellano *et al.*, 2015). Bisulfite sequencing of DNA obtained from viroid-infected cucumber plants infiltrated with empty vectors clearly correlated the HSVd infection with reduced cytosine methylation in a key promoter region of cucumber 45S rDNA, reinforcing our previous observation that HSVd infection and hypomethylation of ribosomal genes occur in parallel in this viroid host. However, a significant increase in the methylation levels of this regulatory rDNA region was observed when recombinant HDA6 was overexpressed in the leaves of these same HSVd-infected plants. Furthermore, the modifications in the methylation levels of cytosine residues in the symmetric sequence context were also observed when cucumber HDA6 was transiently overexpressed in viroid-infected *N. benthamiana* plants. The demonstration that overexpression of exogenous cucumber HDA6 could reverse, at least in part, the dynamic changes in rDNA methylation induced by viroid infection in cucumber and *N. benthamiana* cells suggests that the alterations in cytosine methylation observed in the HSVd-infected plants may be associated with viroid interferences in the HDA6-dependent pathways responsible for the maintenance of rDNA methylation (Earley *et al.*, 2010). We can speculate that the interaction between HSVd and HDA6 interferes with the formation of the HDA6–MET1 complex that is required to regulate maintenance of DNA methylation in symmetric sequence contexts (To *et al.*, 2011; Liu *et al.*, 2012a,b). Further studies will be necessary to determine whether viroid-mediated recruitment of HDA6 also affects cytosine methylation in alternative HDA6 targets, such as repetitive DNA encoding transposable elements (Liu *et al.*, 2012a,b).

Altogether, these data support that HSVd is able to recruit and functionally inactivate host HDA6 during infection, consequently inducing changes in the methylation status of rDNA and causing transcriptional reactivation of normally silenced rRNA genes. Moreover, and in response to this functional interaction, there is increased accumulation of HDA6 in the nuclei of infected cells during the first steps of the infectious process. These findings support the view that epigenetic regulation of host transcriptional activity constitutes a regulatory mechanism associated with the plant response to viroid infection, as was previously shown for the pathogenesis processes induced by bacteria

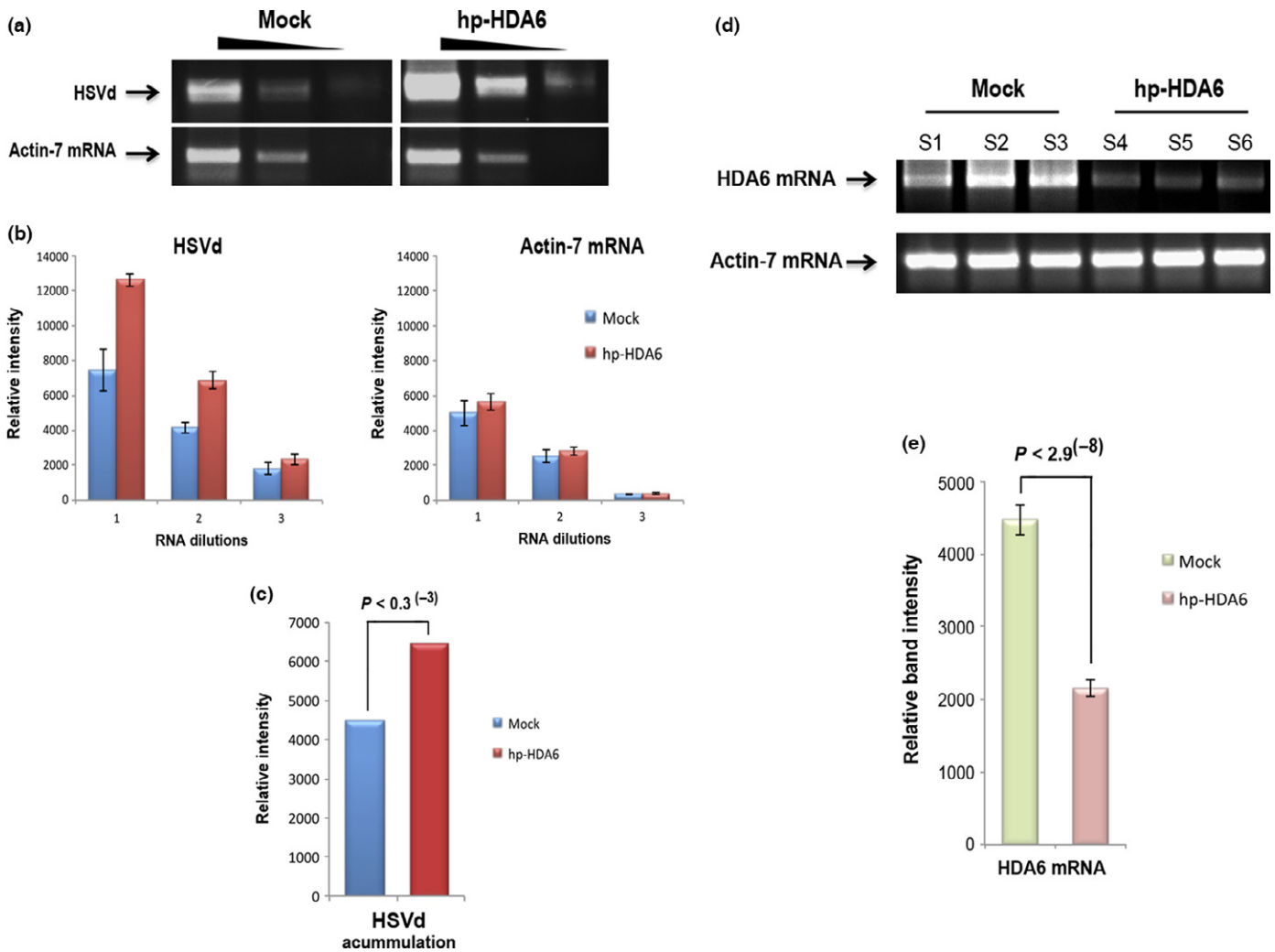

Fig. 5 *Hop stunt viroid* (HSVd) accumulation is increased in cucumber plants with reduced Histone Deacetylase 6 (HDA6) expression. (a) Representative RT-PCR analyses of the viroid accumulation in serial dilutions of total RNAs extracted from infected cotyledons overexpressing a hairpin construct designed to silence the gene encoding HDA6 (hp-HDA6) or mock infiltrated with empty vector. RT-PCR amplification of ubiquitin-40S ribosomal protein mRNA served as a RNA loading control. (b) Histogram showing the comparison between the relative intensity of the bands amplified by RT-PCR from the dilutions of the RNAs extracted from infected plants infiltrated with hp-HDA6 and empty plasmid, respectively. The values obtained for the RT-PCR products of ubiquitin mRNA (control) were also analyzed. The bars (red for HSVd/hp-HDA6 and blue for HSVd/Mock) represent the means of three biological and three technical replicates, ± SE of the means. (c) Comparison of relative HSVd accumulation (estimated as in Fig. 4) in HDA6-silenced and mock-infiltrated samples. Bars (red for HSVd/hp-HDA6 and blue for HSVd/Mock) represent the mean values obtained for HSVd RNA amplification expressed relative to control. Paired *t*-test values: HSVd mean values 4468 (HSVd/mock) and 6442 (HSVd/hp-HDA6). The *P*-value is shown in the figure. (d) Representative RT-PCR analyses of the HDA6 mRNA levels in total RNAs extracted at 4 d post infiltration from three cucumber cotyledons infiltrated with *Agrobacterium* transformed with the vector hp-HDA6 (S4 to S6) and three mock-infiltrated controls (S1–S3). RT-PCR amplification of actin seven mRNA served as an RNA loading control. (e) Histogram showing the comparison between the relative HDA6 mRNA levels estimated by RT-PCR in HDA6-silenced and mock-infiltrated samples. Bars (red for hp-HDA6 and green for mock) represent the mean values obtained for HDA6 mRNA amplification expressed relative to control. Paired *t*-test values: HDA6 mean values 4458 (mock) and 2146 (hp-HDA6), ± SE. The *P*-value is shown in the figure.

(Dowen *et al.*, 2012; Yu *et al.*, 2013) and viruses (Raja *et al.*, 2008; Rodriguez Negrete *et al.*, 2013; Yang *et al.*, 2013).

However, a fundamental question remains unanswered: does the interaction between HSVd and HDA6 provide any adaptive advantage for viroids? Analysis of the HSVd accumulation estimated by RT-PCR revealed that viroid levels were reduced significantly when exogenous HDA6 was transiently overexpressed in infected cucumber and *N. benthamiana* plants. This suggests that an excess of free HDA6 in the nuclei of infected cells negatively affects the accumulation of HSVd, providing evidence for a functional link between HDA6 activity and viroid biological efficiency. This idea was reinforced by the observation that transient silencing of cucumber HDA6 favors HSVd accumulation in infected plants.

Speculations regarding the functional nature of the HSVd–HDA6 complex during viroid infection seem premature at this point. However, it is opportune to consider that, although it is well established that members of the *Pospiviroidae* family recruit and re-direct RNA Pol II to transcribe the viroid RNA instead of the host DNA template (Flores & Semancik, 1982; Mühlbach &

Sänger, 1997; Bojic *et al.*, 2012), the strategy used by these pathogenic lncRNAs to reprogram RNA Pol II activity remains a conundrum. Interestingly, it was previously shown in *Arabidopsis hda6* mutants that, in addition to hypomethylation, loss of HDA6 activity was associated with spurious Pol II transcription of nonconventional rDNA templates (normally transcribed by RNA Pol I) (Earley *et al.*, 2010). Based on these observations, we envision a hypothetical scenario in which, subsequent to cell invasion and once localized in the nucleus, HSVd RNA recruits and functionally inactivates endogenous HDA6 to promote spurious RNA Pol II activity, as indicated by the overaccumulation of pre-rRNAs and rb-sRNAs in infected plants (Martinez *et al.*, 2014; Castellano *et al.*, 2015). This favorable transcriptional environment may promote RNA Pol II to recognize and spuriously transcribe noncanonical templates (viroid RNA) in a manner similar to that observed for rDNA intergenic regions in *Arabidopsis hda6* mutants (Earley *et al.*, 2010). Further studies assessing the stability of the HSVd-RNA Pol II complex in relation to HDA6 accumulation in viroid-infected plants are required to shed light on this possibility.

In summary, the data reported herein reveal that HSVd is able to recruit and subvert host HDA6 during infection, providing novel evidence regarding the potential of viroids to redesign the host cell environment and reprogram host regulatory mechanisms to ensure that their infectious cycle can be fulfilled. Furthermore, this study provides additional support to the emerging idea that the study of viroids as regulatory elements capable of altering host cell homeostasis can contribute to interpret the poorly understood pan-regulatory pathways directed by lncRNAs in plants (Ding, 2010; Gomez & Pallas, 2013; Katsarou *et al.*, 2015; Liu *et al.*, 2015; Gago-Zachert, 2016).

Acknowledgements

The authors thank Dr M. Fares for the contribution to the statistical analysis of the data and Dr G. Martinez for the critical reading of this manuscript.

Author contributions

M.C. performed the experiments, discussed the results and revised the manuscript. V.P. discussed the results and wrote the main manuscript text. G.G. designed the experiments, discussed the results, prepared figures and wrote the main manuscript text.

References

Adkar-Purushothama CR, Brosseau C, Giguère T, Sano T, Moffettb P, Perreault JP. 2015. Small RNA derived from the virulence modulating region of the potato spindle tuber viroid silences callose synthase genes of tomato plants. *Plant Cell* **27**: 2178–2194.

Aufsatz W, Mette M, van der Winden J, Matzke M, Matzke AJ. 2002. HDA6, a putative histone deacetylase needed to enhance DNA methylation induced by double-stranded RNA. *EMBO Journal* **21**: 6832–6841.

Bojic T, Beeharry Y, Zhang DJ, Pelchat M. 2012. Tomato RNA polymerase II interacts with the rod-like conformation of the left terminal domain of the potato spindle tuber viroid positive RNA genome. *Journal of General Virology* **93**: 1591–1600.

Castellano M, Martinez G, Pallás V, Gómez G. 2015. Alterations in host DNA methylation in response to constitutive expression of Hop stunt viroid RNA in *Nicotiana benthamiana* plants. *Plant Pathology* **64**: 1247–1257.

Dalakouras A, Dadami E, Bassler A, Zwiebel M, Krczal G, Wassenegger M. 2015. Replicating Potato spindle tuber viroid mediates *de novo* methylation of an intronic viroid sequence but no cleavage of the corresponding pre-mRNA. *RNA Biology* **12**: 268–275.

Dalakouras A, Wassenegger M. 2013. Revisiting RNA-directed DNA methylation. *RNA Biology* **10**: 453–455.

Ding B. 2010. Viroids: self-replicating, mobile, and fast-evolving noncoding regulatory RNAs. *Wiley Interdisciplinary Reviews RNA* **1**: 362–375.

Dowen R, Pelizzola M, Schmitz R, Lister R, Dowen JM, Nery JR, Dixon JE, Ecker JR. 2012. Widespread dynamic DNA methylation in response to biotic stress. *Proceedings of the National Academy of Sciences, USA* **109**: 2183–2191.

Eamens AL, Smith N, Dennis E, Wassenegger M, Wang MB. 2014. In *Nicotiana* species, an artificial microRNA corresponding to the virulence modulating region of Potato spindle tuber viroid directs RNA silencing of a soluble inorganic pyrophosphatase gene and the development of abnormal phenotypes. *Virology* **450**: 266–277.

Earley KW, Pontvianne F, Wierzbicki AT, Blevins T, Tucker S, Costa-Nunes P, Pontes O, Pikaard CS. 2010. Mechanisms of HDA6-mediated rRNA gene silencing: suppression of intergenic Pol II transcription and differential effects on maintenance versus siRNA-directed cytosine methylation. *Genes Development* **24**: 1119–1132.

Flores R, Gago Zachert S, Serra P, Sanjuán R, Elena SF. 2014. Viroids: survivors from the RNA world? *Annual Review of Microbiology* **68**: 395–414.

Flores R, Semancik JS. 1982. Properties of a cell-free system for synthesis of citrus exocortis viroid. *Proceedings of the National Academy of Sciences, USA* **79**: 6285–6288.

Gago-Zachert S. 2016. Viroids, infectious long non-coding RNAs with autonomous replication. *Virus Research* **212**: 12–24.

Gas ME, Hernández C, Flores R, Daròs JA. 2007. Processing of nuclear viroids *in vivo*: interplay between RNA conformations. *PLoS Pathogens* **3**: e182.

Gomez G, Martinez G, Pallas V. 2008. Viroid-induced symptoms in *Nicotiana benthamiana* plants are dependent on RDR6 activity. *Plant Physiology* **148**: 414–423.

Gomez G, Martinez G, Pallas V. 2009. Interplay between viroid-induced pathogenesis and RNA silencing pathways. *Trends in Plant Science* **14**: 264–269.

Gomez G, Pallas V. 2004. A long-distance translocatable phloem protein from cucumber forms a ribonucleoprotein complex *in vivo* with Hop stunt viroid RNA. *Journal of Virology* **78**: 10 104–10 110.

Gomez G, Pallas V. 2006. Hop stunt viroid is processed and translocated in transgenic *Nicotiana benthamiana* plants. *Molecular Plant Pathology* **7**: 511–517.

Gomez G, Pallas V. 2007. Mature monomeric forms of Hop stunt viroid resists RNA silencing in transgenic plants. *Plant Journal* **51**: 1041–1049.

Gomez G, Pallas V. 2013. Viroids: a light in the darkness of the lncRNA-directed regulatory networks in plants. *New Phytologist* **198**: 10–15.

Gomez G, Torres H, Pallás V. 2005. Identification of translocatable RNA-binding phloem proteins from melon, potential components of the long-distance RNA transport system. *Plant Journal* **41**: 107–116.

Hristova E, Fal K, Klemme L, Windels D, Bucher E. 2015. HDA6 controls gene expression patterning and DNA methylation-independent euchromatic silencing. *Plant Physiology* **168**: 1298–1308.

Katsarou K, Rao AL, Tsagris M, Kalantidis K. 2015. Infectious long non-coding RNAs. *Biochimie* **117**: 37–47.

Li LC, Dahiya R. 2002. MethPrimer: designing primers for methylation PCRs. *Bioinformatics* **18**: 1427–1431.

Liu X, Hao L, Li D, Zhu L, Hu S. 2015. Long non-coding RNAs and their biological roles in plants. *Genomics Proteomics Bioinformatics* **13**: 137–147.

Liu X, Luo M, Wu K. 2012a. Epigenetic interplay of histone modifications and DNA methylation mediated by HDA6. *Plant Signaling Behavior* **7**: 633–635.

Liu X, Yu C, Duan J, Luo M, Wang K, Tian G, Cui Y, Wu K. 2012b. HDA6 directly interacts with DNA methyltransferase MET1 and maintains transposable element silencing in Arabidopsis. *Plant Physiology* **158**: 119–129.

Martinez G, Castellano M, Tortosa M, Pallas V, Gomez G. 2014. A pathogenic non-coding RNA induces changes in dynamic DNA methylation of ribosomal RNA genes in host plants. *Nucleic Acids Research* **42**: 1553–1562.

May B, Lippman Z, Fang Y, Spector D, Martienssen RA. 2005. Differential regulation of strand-specific transcripts from Arabidopsis centromeric satellite repeats. *PLoS Genetics* **1**: e79.

Mühlbach HP, Sänger HL. 1997. Viroid replication is inhibited by alpha-amanitin. *Nature* **278**: 185–188.

Navarro B, Gisel A, Rodio ME, Delgado S, Flores R, Di Serio F. 2012a. Viroids: how to infect a host and cause disease without encoding proteins. *Biochimie* **94**: 1474–1480.

Navarro B, Gisel A, Rodio M, Delgado S, Flores R, Di Serio F. 2012b. Small RNAs containing the pathogenic determinant of a chloroplast-replicating viroid guide the degradation of a host mRNA as predicted by RNA silencing. *Plant Journal* **70**: 991–1003.

Navarro JA, Vera A, Flores RA. 2000. Chloroplastic RNA polymerase resistant to tagetitoxin is involved in replication of avocado sunblotch viroid. *Virology* **268**: 218–225.

Nohales MA, Flores R, Daros JA. 2012b. Viroid RNA redirects host DNA ligase 1 to act as an RNA ligase. *Proceedings of the National Academy of Sciences, USA* **109**: 13 805–13 810.

Nohales MA, Molina Serrano D, Flores R, Daros JA. 2012a. Involvement of the chloroplastic isoform of tRNA ligase in the replication of viroids belonging to the family Avsunviroidae. *Journal of Virology* **86**: 8269–8276.

Owens RA, Hammond RW. 2009. Viroid pathogenicity: one process, many faces. *Viruses* **1**: 298–316.

Palukaitis P. 2014. What has been happening with viroids? *Virus Genes* **49**: 175–184.

Papaefthimiou I, Hamilton A, Denti M, Baulcombe D, Tsagris M, Tabler M. 2001. Replicating potato spindle tuber viroid RNA is accompanied by short RNA fragments that are characteristic of post-transcriptional gene silencing. *Nucleic Acids Research* **29**: 2395–2400.

Probst A, Fagard M, Proux F, Mourrain P, Boutet S, Earley K, Lawrence RJ, Pikaard CS, Murfett J, Furner I *et al.* 2004. Arabidopsis Histone Deacetylase HDA6 is required for maintenance of transcriptional gene silencing and determines nuclear organization of rDNA repeats. *Plant Cell* **16**: 1021–1034.

Raikhel N. 1992. Nuclear targeting in plants. *Plant Physiology* **100**: 1627–1632.

Raja P, Sanville BC, Buchmann R. 2008. Viral genome methylation as an epigenetic defense against geminiviruses. *Journal of Virology* **82**: 8997–9007.

Ricardi M, González RM, Iusem ND. 2010. Protocol: fine-tuning of a Chromatin Immunoprecipitation (ChIP) protocol in tomato. *Plant Methods* **9**: 6–11.

Rodriguez Negrete E, Lozano Duran R, Piedra Aguilera A, Cruzado L, Bejarano E, Castillo AG. 2013. Geminivirus Rep protein interferes with the plant DNA methylation machinery and suppresses transcriptional gene silencing. *New Phytologist* **199**: 464–475.

Sikorskaite S, Rajamäki ML, Baniulis D, Stanys V, Valkonen JP. 2013. Protocol: optimised methodology for isolation of nuclei from leaves of species in the Solanaceae and Rosaceae families. *Plant Methods* **26**: 9–31.

To T, Kim J, Matsui A, Kurihara Y, Morosawa T, Ishida J, Tanaka M, Endo T, Kakutani T, Toyoda T *et al.* 2011. *Arabidopsis* HDA6 regulates locus-directed heterochromatin silencing in cooperation with MET1. *PLoS Genetics* **7**: e1002055.

Wang MB, Bian XY, Wu LM, Lium LX, Smith N, Isenegger D, Wu RM, Masuta C, Vance VB, Watson JM *et al.* 2004. On the role of RNA silencing in the pathogenicity and evolution of viroids and viral satellites. *Proceedings of the National Academy of Sciences, USA* **101**: 3275–3280.

Yang LP, Fang Y, An CP. 2013. C2-mediated decrease in DNA methylation, accumulation of siRNAs, and increase in expression for genes involved in defense pathways in plants infected with beet severe curly top virus. *Plant Journal* **73**: 910–917.

Yu A, Lepere G, Jay F, Wang J, Bapaume L, Wang Y, Abraham AL, Penterman J, Fischer RL, Voinnet O *et al.* 2013. Dynamics and biological relevance of DNA demethylation in Arabidopsis antibacterial defence. *Proceedings of the National Academy of Sciences, USA* **110**: 2389–2394.

Supporting Information

Additional Supporting Information may be found online in the Supporting Information tab for this article:

Fig. S1 Purification of recombinant cucumber HDA6 and production of polyclonal antiserum.
Fig. S2 HDA6-GFP accumulates specifically in the nucleus of *N. benthamiana* cells.
Fig. S3 Recombinant cucumber HDA6 is detected in nuclear extracts of *N. benthamiana* plants.
Fig. S4 Differential detection of endogenous HDA6 in HSVd-infected plants.
Fig. S5 Cucumber HDA6 binds HSVd–RNA in HSVd-expressing transgenic *N. benthamiana* plants.
Fig. S6 Schematization of combined agro-infiltration assays in infected cucumber and *N. benthamiana* plants.
Fig. S7 Recombinant cucumber HDA6 reverts the hypomethylation induced by HSVd infection in *N. benthamiana* 45S rRNA genes.
Fig. S8 Schematization of transient HDA6 silencing assays in HSVd-infected cucumber plants.

Please note: Wiley Blackwell are not responsible for the content or functionality of any supporting information supplied by the authors. Any queries (other than missing material) should be directed to the *New Phytologist* Central Office.

Author Query Form

Journal: NPH

Article: 14001/2016-21561

Dear Author,
During the copy-editing of your paper, the following queries arose. Please respond to these by marking up your proofs with the necessary changes/additions. Please write your answers on the query sheet if there is insufficient space on the page proofs. Please write clearly and follow the conventions shown on the attached corrections sheet. If returning the proof by fax do not write too close to the paper's edge. Please remember that illegible mark-ups may delay publication.

Many thanks for your assistance.

Query reference	Query	Remarks
1	**AUTHOR: Please confirm that given names (red) and surnames/family names (green) have been identified correctly.**	
2	**AUTHOR: Palukaitis et al., 2014 has been changed to Palukaitis, 2014 so that this citation matches the Reference List. Please confirm that this is correct.**	
3	**AUTHOR: Navarro et al., 2012 has been changed to Navarro et al., 2012a, 2012b so that this citation matches the Reference List. Please confirm that this is correct.**	
4	**AUTHOR: Nohales et al., 2012 has been changed to Nohales et al., 2012a, 2012b so that this citation matches the Reference List. Please confirm that this is correct.**	
5	**AUTHOR: Novagen: please give manufacturer town, state (if USA) and country**	
6	**AUTHOR: Amersham-Pharmacia Biotech, Amersham, UK: address still OK as now part of GE Healthcare?**	
7	**AUTHOR: Fermentas: pleas give manufacturer town (state), country**	
8	**AUTHOR: Please give address information for "Leica": town, state (if applicable), and country.**	
9	**AUTHOR: Liu et al. 2012 has been changed to Liu et al., 2012a, 2012b so that this citation matches the Reference List. Please confirm that this is correct.**	
10	**AUTHOR: Figure 1 is of insufficient resolution; please supply a new file for this figure. The specifications for artwork are available at http://authorservices.wiley.com/bauthor/illustration.asp**	
11	**AUTHOR: Figure 2 is of insufficient resolution; please supply a new file for this figure. The specifications for artwork are available at http://authorservices.wiley.com/bauthor/illustration.asp**	
12	**AUTHOR: Figure 3 is of insufficient resolution; please supply a new file for this figure. The specifications for artwork are available at http://authorservices.wiley.com/bauthor/illustration.asp**	
13	**AUTHOR: Figure 4 is of insufficient resolution; please supply a new file for this figure. The specifications for artwork are available at http://authorservices.wiley.com/bauthor/illustration.asp**	

14	**AUTHOR: Figure 5 is of insufficient resolution; please supply a new file for this figure. The specifications for artwork are available at http://authorservices.wiley.com/bauthor/illustration.asp**	